ELSEVIER

Nuclear Instruments and Methods in Physics Research A 463 (2001) 275–287

NUCLEAR INSTRUMENTS & METHODS IN PHYSICS RESEARCH Section A

www.elsevier.nl/locate/nima

Absolute measurements of the response function of an NE213 organic liquid scintillator for the neutron energy range up to 206 MeV

Noriaki Nakao[a,*], Tadahiro Kurosawa[b,1], Takashi Nakamura[b], Yoshitomo Uwamino[c]

[a] *High Energy Accelerator Research Organization (KEK), Oho, Tsukuba, Ibaraki 305-0801, Japan*
[b] *Department of Quantum Science and Energy Engineering, Tohoku University, Sendai, Miyagi 980-8579, Japan*
[c] *The Institute of Physical and Chemical Research (RIKEN), Wako, Saitama 351-0198, Japan*

Received 10 July 2000; received in revised form 4 November 2000; accepted 7 November 2000

Abstract

The absolute values of the neutron response functions of a 12.7 cm diameter by 12.7 cm long NE213 organic liquid scintillator were measured using a quasi-monoenergetic neutron field in the energy range of 66–206 MeV via the $^{7}Li(p,n)^{7}Be$ reaction in the ring cyclotron facility at RIKEN. The measured response functions were compared with calculations using a Monte Carlo code developed by Cecil et al. The measurements clarified that protons escaping through the scintillator wall induced by high-energy neutrons increase from 6% for 66 MeV neutrons to 35% for 206 MeV neutrons, and that this wall effect causes a difficult problem for n–γ discrimination. Measured response functions without the wall-effect events were also obtained by eliminating the escaping-proton events in the analysis, and compared with calculations using a modified Monte Carlo code. Comparisons between the measurements and calculations both with and without any wall-effect events gave a good agreement, but some discrepancy in the light output distribution could be found, mainly because the deuteron generation process was not taken into account in the calculation. The calculated efficiencies for 10 MeVee threshold, however, also gave good agreement within about 10% with the measurements.

Keywords: Organic liquid scintillator; Response function; Quasi-monoenergetic neutron; $^{7}Li(p,n)^{7}Be$; Wall effect; Monte Carlo calculation

1. Introduction

Recent progress of accelerator technology has made it possible to accelerate high-energy, high-intensity hadrons, which has increased the shield thickness required to reduce the leakage of

*Corresponding author. Tel.: +81-298-79-6004; fax: +81-298-64-4051.
E-mail address: noriaki.nakao@kek.jp (N. Nakao).
[1] Current address: Electrotechnical Laboratory (ETL), Umezono 1-1-4, Tsukuba, Ibaraki 305-8568, Japan

0168-9002/01/$ - see front matter
PII: S0168-9002(01)00260-1

radiation, especially high-energy neutrons having high penetrability. The high-energy neutron spectrometry in such facilities, therefore, has become more important in order to accurately estimate radiation damage to instruments, activation to accelerator and shielding materials, and external exposure to humans due to high-energy neutrons.

For neutron spectrometry above the MeV energy region, organic liquid scintillators, such as NE213 and BC501A, are widely used, combined with a time-of-flight method and an unfolding method. A number of experimental studies of the detector efficiencies and response functions for neutrons below 20 MeV have been conducted; one of the most accurate response functions of the NE213 scintillator has been measured by Verbinski et al. [1]. Thus, in this energy range, the response functions can now be well reproduced by Monte Carlo calculations. On the other hand, in an energy range above 20 MeV, several measurements of the response functions in the several-tens-MeV neutron energy region have been reported [2–4]. Recently, response functions of an NE213 in the neutron energy range up to 133 MeV have been measured [5], and compared with Monte Carlo calculations using the SCINFUL code [6] and a code by Cecil et al. [7] (CECIL code), which have clarified some discrepancy between measurements and calculations. Moreover, the data of light yields for protons and deuterons in the NE213 scintillator were newly parameterized [5]. The response functions of BC501 and NE213 for neutrons of energy up to 492 MeV have been measured by Sailor and Byrd [8,9], but the experimental data for neutron energies higher than 100 MeV are very scarce.

For high-energy neutrons, a wall effect of the scintillator can not be neglected, since the probability of neutron-induced charged particles escaping from the detector wall increases, and these escaping protons can be rejected in a process of n-γ discrimination, since the pulse shape of the escaped particles becomes closer to that of γ-ray-induced electrons. We have already pointed out the fact of an efficiency decrease due to the wall effect, and calculated the efficiencies without escaping protons by a modified CECIL code for high-energy-neutron measurements at RIKEN [10] and at the Heavy Ion Medical Accelerator (HIMAC), National Institute of Radiological Sciences (NIRS), Japan [11,12].

In this work, the absolute values of response functions for the neutron energy range from 66 to 206 MeV were measured using quasi-monoenergetic neutron sources at the RIKEN ring cyclotron facility (RRC) [10], and were compared with the calculated results in the case of excluding the escaping protons by wall effect.

2. Experiment

2.1. Neutron beam course and neutron source

The absolute values of the response functions of the scintillator were measured using a quasi-monoenergetic neutron field which has been installed at the E4 room in the RIKEN ring cyclotron facility (RRC) [10]. The neutron beam course of the E4 room is illustrated in Fig. 1. The neutrons were produced from a 10 mm-thick ^{7}Li metal target (99.98 atm% enriched, 0.54 g cm^{-3}) bombarded by 70, 80, 90, 100, 110, 120, 135 MeV/n H_2^+-ions or 150, 210 MeV protons. The protons that penetrated the ^{7}Li target were bent by a PD1-dipole-magnet towards the beam dump in the beam duct through PD1, which is insulated for use as a Faraday cup. A cross-sectional view of the neutron beam course at RRC is shown in Fig. 1. The neutrons produced at 0 degree from the target passed through an 3 cm-thick acrylic vacuum window and a 120 cm thick iron collimator having a 22 cm-wide by 22 cm-high hole, and reached the neutron measurement area.

The energy spectra of the quasi-monoenergetic neutrons measured in our previous work by the TOF method using an NE213 organic liquid scintillator [10] is shown in Fig. 2. These quasi-monoenergetic neutron sources form a dominant neutron peak, the energy of which is 3–4 MeV lower than the injected-proton energy, and a lower continuum part generated by spallation reactions.

The peak neutron fluences in the experiment were estimated using two relative neutron fluence monitors, NE213 organic liquid scintillator

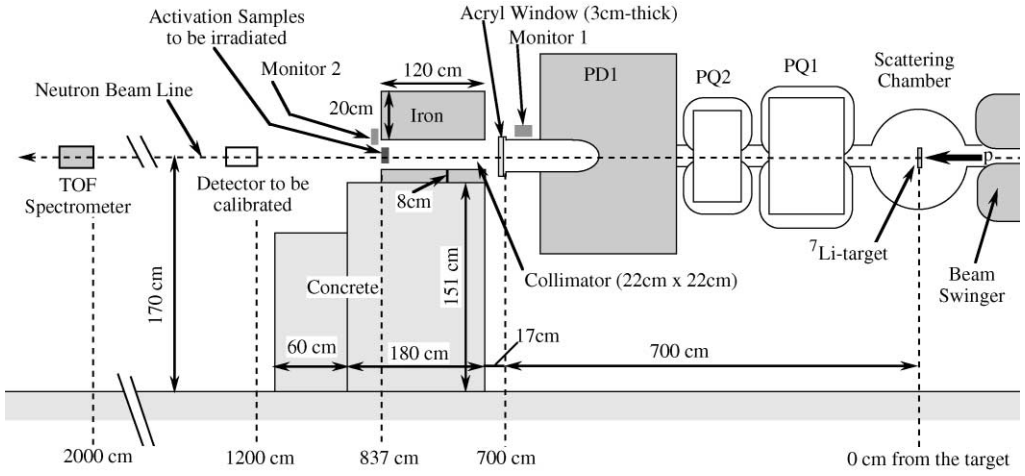

Fig. 1. Experimental setup at the neutron beam course at the E4 room of the RIKEN ring cyclotron facility (RRC).

(5.08 cm diameter × 5.08 cm long) placed near the PD1 magnet (Monitor 1) and NE102A plastic scintillator (2 cm wide × 2 cm high × 0.5 cm thick) at the collimator exit (Monitor 2), as shown in Fig. 1. The counts of these neutron fluence monitors were calibrated to the absolute monoenergetic peak neutron fluence on the beam line by measuring 478 keV γ-rays from ^{7}Be nuclei produced in an ^{7}Li target through the ^{7}Li(p, n)^{7}Be (g.s. + 0.429 MeV) reaction [10]. The error of the fluence monitor is 9.0% for the peak neutron fluence, 12 m from the target [10]. Since the measurement of the total number of protons using the current integrator through the beam dump has an uncertainty in a low-current experimental run, the neutron fluences can be measured more accurately by this target activity measurement.

2.2. Experimental set-up

Using the quasi-monoenergetic neutron source, the response functions of a 12.7 cm diameter by 12.7 cm long NE213 organic liquid scintillator (Nuclear Enterprise Co. Ltd.) were measured. The density and the composition of the scintillator are 0.874 g cm^{-3} and $CH_{1.213}$, respectively. This scintillator is coupled to a R4144 photomultipiler connected to the E1458 base (Hamamatsu Photonics Co. Ltd.) [5].

The detector was placed on the neutron beam line at 12 m from the ^{7}Li target, as shown in Fig. 1. The response functions for the peak neutron energies were measured using the time-of-flight (TOF) method, and the repetition period of the proton beam from the cyclotron was extended to about 1.0 μs by using a beam chopper to avoid any contamination of lower energy neutrons in the peak neutron region of the neutron-flight-time distribution. In the measurements, the currents of the proton beam were kept in the range of 0.5–2 nA.

The electronic circuits shown in Figs. 3(a) and (b) were used for response-function measurements. In a measurement using circuit (a), charges of the dynode signals were integrated by the pre-amplifier (PA) and amplified with the delay-line amplifier (DLA). Output pulses from the DLA were input separately into the delay amplifier (DA) and the rise-time-to-height converter (RHC). The pulse-heights of the outputs from DA and RHC correspond to total pulse-area (total light output) and decay time of the detector signal, respectively, and were used for the two-dimensional discrimination of neutron and γ-ray events. The neutron flight-time was measured with the anode signals from the detector as start signals and the trigger pulses of the beam chopper as stop signals. These three pulses were digitized by a CAMAC ADC

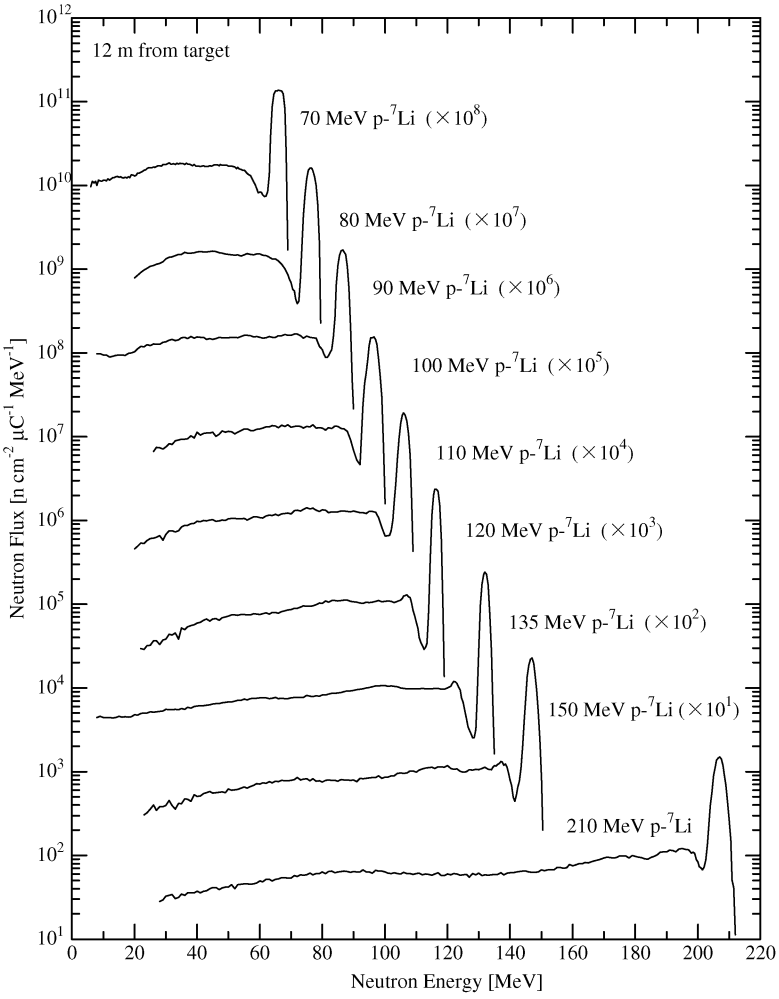

Fig. 2. Energy spectra of quasi-monoenergetic neutron sources generated from 10 mm thick ^{7}Li target bombarded by protons at RIKEN ring cyclotron facility, which were used for the response-function measurement.

and recorded in an event-by-event mode by the VAX data-taking system.

In order to extend the dynamic range of the light output distribution, the electronic circuit shown in Fig. 3(b) was employed in recent measurements for 70, 90 and 135 MeV p-^{7}Li neutrons. By using this circuit, a much lower light output of the response function than that by circuit (a) could be measured. By using the QDC (charge ADC), the charges of the total pulse-area and slow (decay) components of the anode pulses were integrated for particle identification. The neutron flight time was measured by a time-to-digital converter (TDC). These three digital data from the CAMAC QDC and TDC were stored in a personal computer. All of these processes were controlled by the KODAQ data-taking system (Kakuken Online Data Aquisition System) [13].

3. Analysis

The absolute flight time of neutrons was determined using the γ-ray peak flashed from the

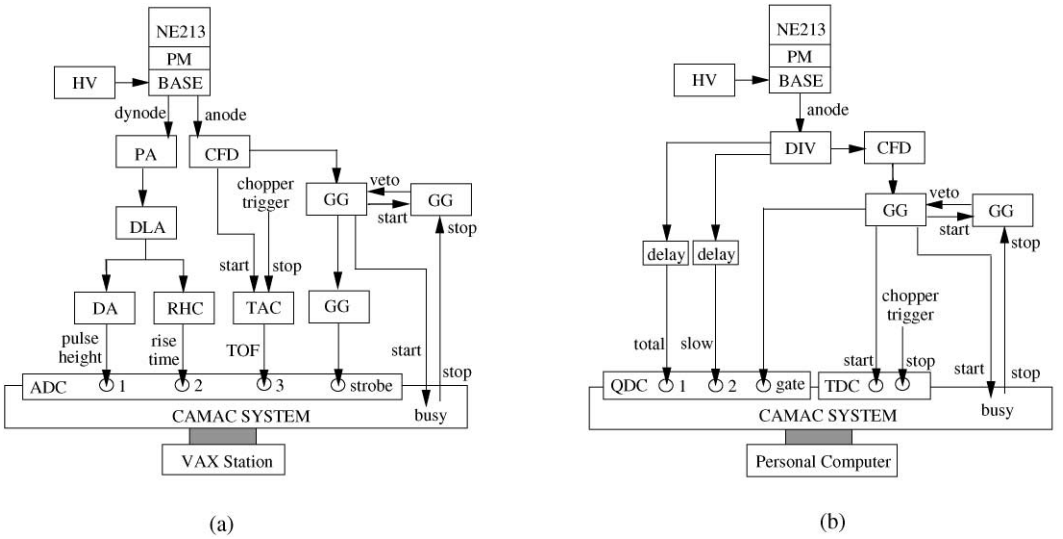

Fig. 3. Block diagrams of (a) old and (b) new circuits for the TOF measurement using the NE213 scintillator. PM: photomultiplier, HV: high voltage power supply (John Fluke), PA: pre-amplifier (ORTEC 113), CFD: constant fraction discriminator (ORTEC 935), DLA: delay line amplifier (ORTEC 460), DA: delay amplifier (ORTEC 427A), RHC: rise-time-to-height converter (OKEN 7231C), TAC: time-to-amplitude converter (ORTEC 567), GG: gate and delay generator (KAIZU 1500), ADC: analog-to-digital converter (ORTEC AD811), DIV: signal divider, QDC: charge analog-to-digital converter (LeCroy 2249W), TDC: time-to-digital converter (LeCroy 2228A).

^{7}Li target, and the TOF distribution was converted to the energy spectrum using the relativistic kinematics. The light output distributions for monoenergetic peak neutrons were selected from the obtained neutron energy spectra.

Figs. 4(a) to (d) show two-dimensional distributions of the rise-time versus the light output for 35, 80, 150 and 210 MeV p-^{7}Li neutrons which were obtained with the circuit shown in Fig. 3(a). The distribution of 35 MeV p-^{7}Li neutrons shown in Fig. 4(a) is cited from Ref. [5] to compare with the other three higher energy neutron sources. The p, d and α particles were produced from neutrons, and the electrons were from γ-rays in the scintillator. Although most of the generated charged particles are clearly identified in the figures, the electron components generated from γ-rays overlap with high energy protons which escaped from the scintillator wall (escaping proton) for 80, 150 and 210 MeV neutrons in the figures. The amount of escaping protons cannot be neglected for high-energy neutrons, compared with the total response functions, as shown in the figure.

The lowest light output, where the electron component could be distinguished from the escaping protons, was around 10 MeV-electron-equivalent (MeVee) in this work. The electron component was eliminated from the distribution, and the total response functions were estimated for a light output higher than 10 MeVee. In fact, the higher part of the electron component almost consists of muons due to cosmic rays, and the contribution above 10 MeVee was less than 0.1% of the total response function. To reduce the response function to as low an energy as possible, both the electron and escaping-proton components were eliminated from the two-dimensional distributions, then the one-dimensional light output distributions without escaping protons were obtained by summing all other components.

By using the circuit shown in Fig. 3(b), the two-dimensional distribution of slow pulse component versus the total pulse-area for 135 MeV p-^{7}Li neutrons is shown in Fig. 5. Since the dynamic range of the measured pulse area is wider than that of the circuit in Fig. 3(a), the pulse area could be

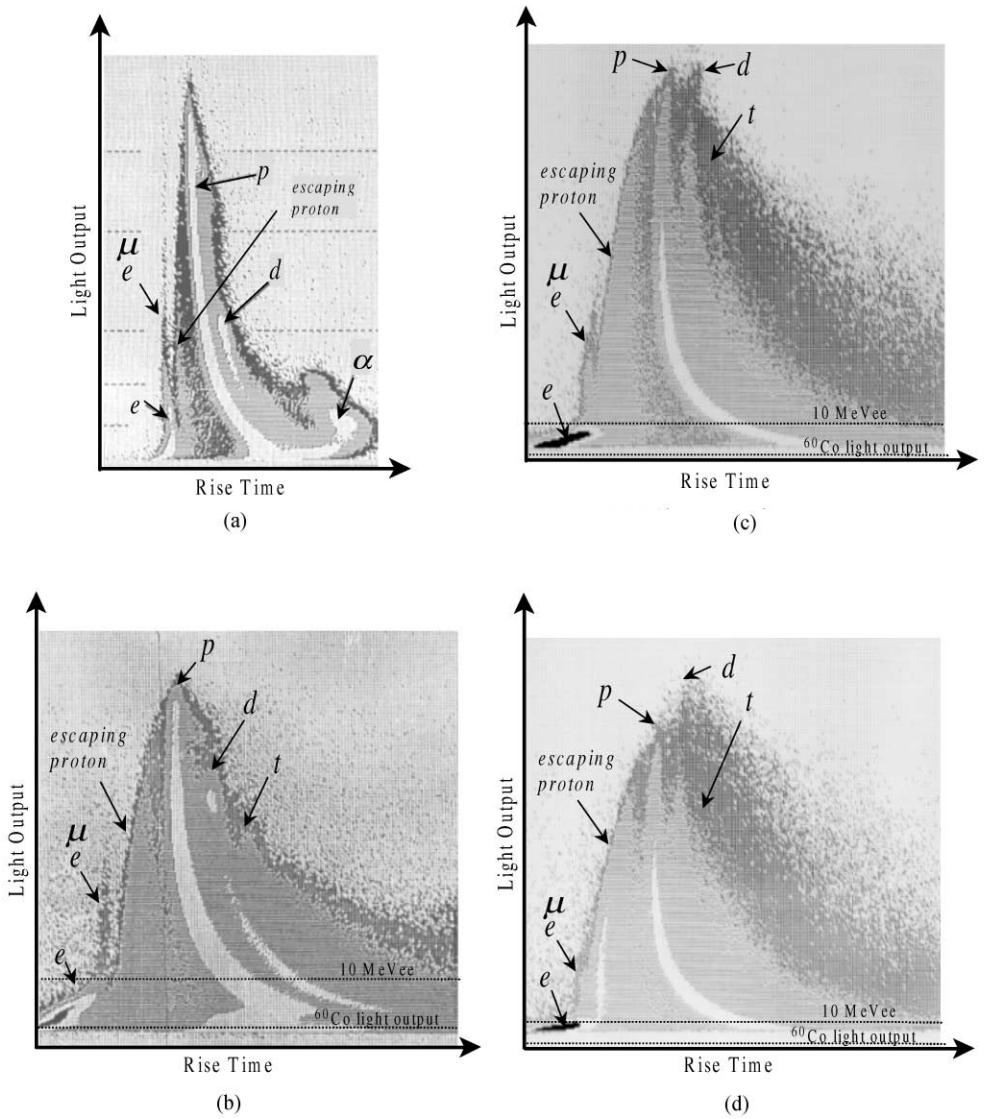

Fig. 4. Two-dimensional plots of rise-time versus light output using the measuring circuit in Fig. 3(a) to identify the particles produced in the scintillator for (a) 35 MeV [5], (b) 80 MeV, (c) 150 MeV and (d) 210 MeV p-^{7}Li neutron source. The α particles are not shown in (b) to (d) in order to expand the escaping-proton area.

measured down to ^{60}Co-equivalent light output. In addition, the events of p, d, and α particles stopped in the detector can be clearly distinguished from the electron and escaping-proton events, as shown in the figure. The electron component, however, could not be distinguished from the escaping-proton components, even above 10 MeVee. Although the contribution of electron and muon events above 10 MeVee, which can be neglected in this work, were not eliminated, the total response functions including escaping-proton events above 10 MeVee were obtained. On the other hand, by eliminating both electron and escaping-proton events, the response functions without escaping protons could be obtained down to ^{60}Co light output.

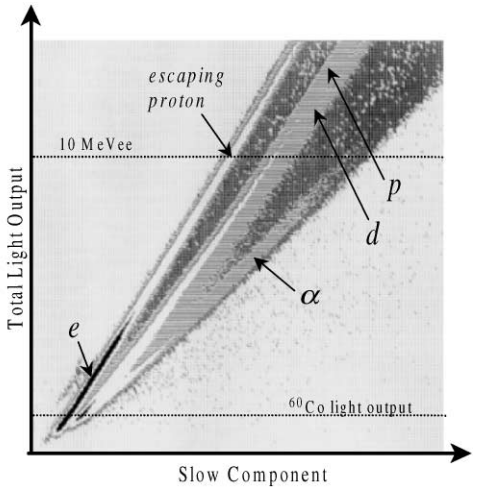

Fig. 5. Two-dimensional plots of the slow component versus the total pulse-area (light output) using the measuring circuit in Fig. 3(b) to identify the particles produced in the scintillator for 135 MeV p-^{7}Li neutron source (expanded in the low light output part).

An energy calibration was performed in all measurements to convert the light outputs into MeVee by using the reference light output as follows. The ^{60}Co light output corresponding to 1.15 MeVee was determined to be the channel having 0.303 times the counts of the Compton edge due to 1.17 and 1.33 MeV γ-ray from ^{60}Co. The ^{241}Am–Be light output corresponding to 4.2 MeVee was determined to be the channel having 0.664 times the counts of the Compton edge due to 4.43 MeV γ-ray from ^{241}Am–Be. For the calibration of higher light output, the recoiled proton edge in the light output distribution for the TOF-gated-monoenergetic neutrons was determined using the light yield expressed by Eq. (3) of Ref. [5]. In addition, the light output of deuteron peak in the neutron response functions was also utilized for a higher light output calibration using Eqs. (3) and (4) of Ref. [5].

4. Monte Carlo calculations

To calculate the response function and efficiency for high-energy neutrons up to around 1 GeV, a Monte Carlo code developed by Cecil et al. (CECIL code) [7] is widely used. In this work, for a comparison with the measured results, calculations of the response functions were performed with this code. In the calculations, the data of particle range for the PILOT-B scintillator (1.02 g/cm^3), which was compiled in this code, was replaced by that for the NE213 scintillator.

The scintillation light output by protons escaping through a detector wall is generally expressed as

$$L = L(E) - L(E_{\text{escape}}), \tag{1}$$

where L is the actual light output in the scintillator by the charged particle escaping from the detector wall, $L(E)$ is the light output by the charged particle of energy E if it fully deposits its energy in the scintillator, E_{escape} is the energy of the charged particle just after escaping from the detector wall. In this work, the code was modified to calculate the response functions without escaping-proton events. $L = 0$ is given instead of Eq. (1) if the produced charged particle goes out of the detector wall.

5. Results and discussions

5.1. Comparison between measured and calculated response functions

Figs. 6(a) to (i) show the measured response functions for nine peak neutron energies (see Fig. 2), by comparing them with those calculated with the CECIL code. Although slight discrepancies can be found in the structures of the response functions in these figures, the calculations generally give good agreement with the measurements. In Figs. 6(a)–(f), the discrepancy between the measurement and the calculation in the recoiled proton edge of the response function can be seen, and it becomes larger on increasing the neutron energy, because the light yield compiled in the CECIL code is higher than that in the measured data [5]. The proton range of about 120 MeV energy is equivalent to this scintillator size of 12.7 cm length; nevertheless, the maximum light output of the measured and calculated response functions still extend beyond that of 120 MeV

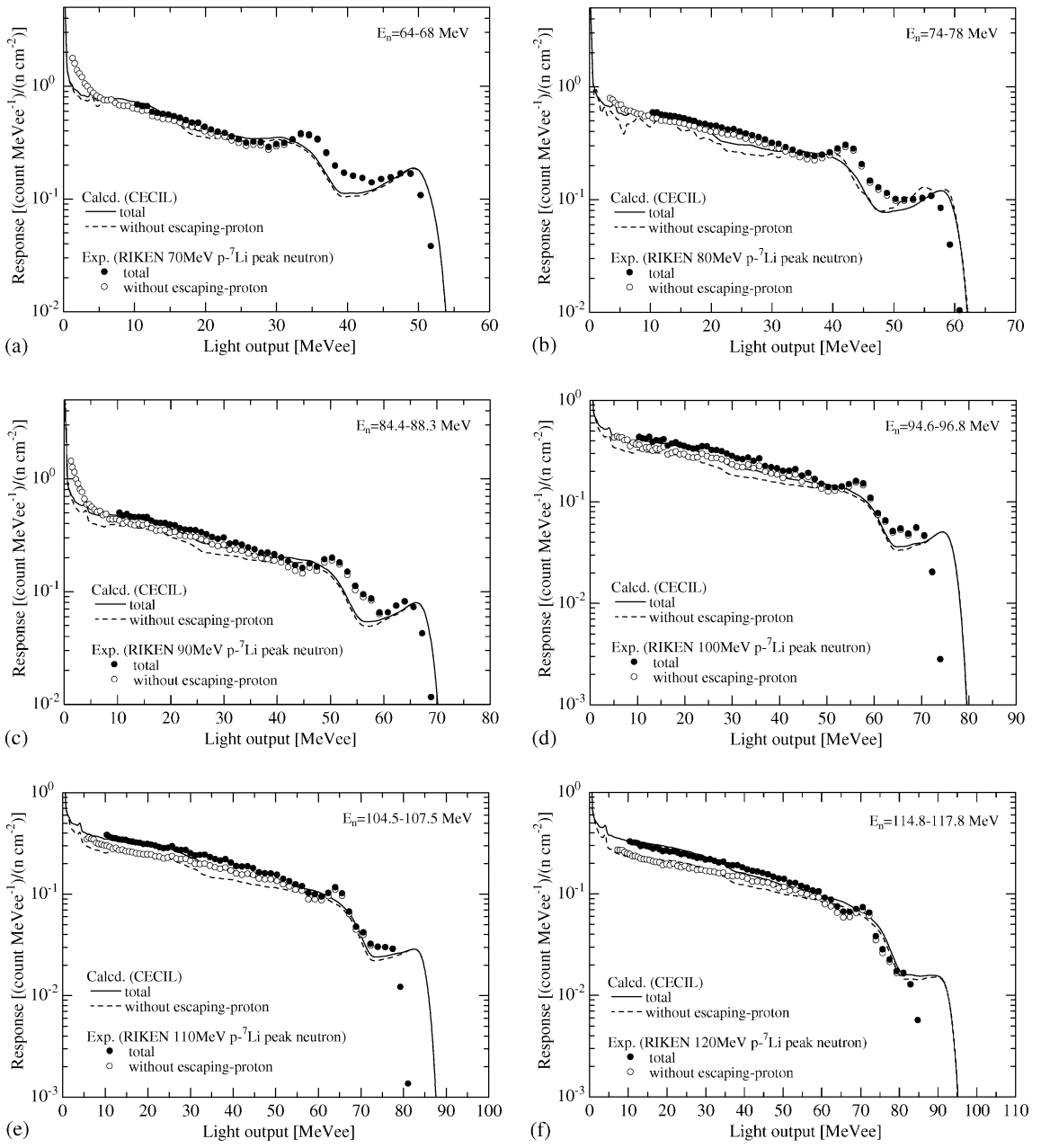

Fig. 6. Measured response functions of NE213 with and without escaping protons compared with the calculations for neutron energy ranges of (a) 64–68 MeV, (b) 74–78 MeV, (c) 84.4–88.3 MeV, (d) 94.6–96.8 MeV, (e) 104.5–107.5 MeV, (f) 114.8–117.8 MeV (g) 131.7–133.3 MeV, (h) 145.6–148.0 MeV, (i) 205.8–207.8 MeV.

protons produced by neutrons of an energy above 120 MeV in Figs. 6(g)–(i). This indicates that neutrons deposit their energy in the scintillator through multiple charged-particle production by multiple scattering and spallation reactions, which produce large amounts of light output. It can also

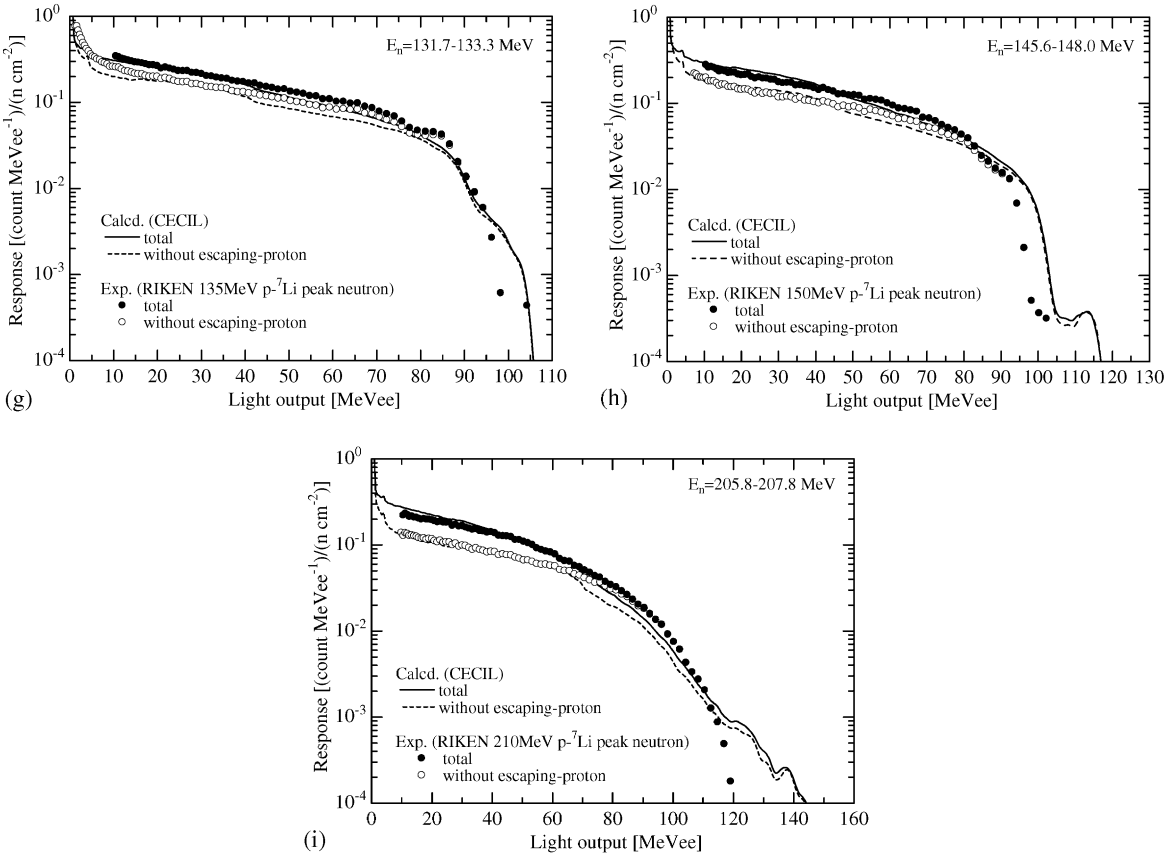

Fig. 6. *Continued*

be considered that a large light output is emitted due to single deuteron production from neutrons above 120 MeV, since the scintillator size is equivalent to a 150 MeV deuteron range.

A broad peak can be found in the middle part of the measured response function for 80 MeV p-^{7}Li neutrons of Fig. 6(b), which is due to deuterons generated by the ^{12}C(n, d) reaction, since a deuteron peak can be seen in the deuteron component of Fig. 4(b). A similar broad peak can also be seen in the calculated response function, but it is formed by particles generated through the ^{12}C(n, np) reaction.

Figs. 7(a)–(d) show comparisons of the measured total response functions and the deuteron component distributions with the summation and components of the calculated light output distributions of particles produced from several neutron reactions in the scintillator. The measured deuteron component in the figures generally agrees in the higher part of light output with the calculated distribution, due to the ^{12}C(n, np) reaction. However, in the lower part, the measured results are much lower than the calculated results. In Fig. 8, the cross-section data of the (n, np) reaction compiled in the CECIL code is compared with the summation of the (n, d), (n, p) and (n, np) reaction cross-section data compiled in the SCINFUL code [6]. Although the deuteron production in the scintillator is not taken into account in the CECIL code, the contribution of deuterons is treated as the (n, np) reaction in the code. This approximation causes a negligible difference in the light output distribution below 100 MeV for the scintillator of this size, since the energy dependences of the light yields for protons and

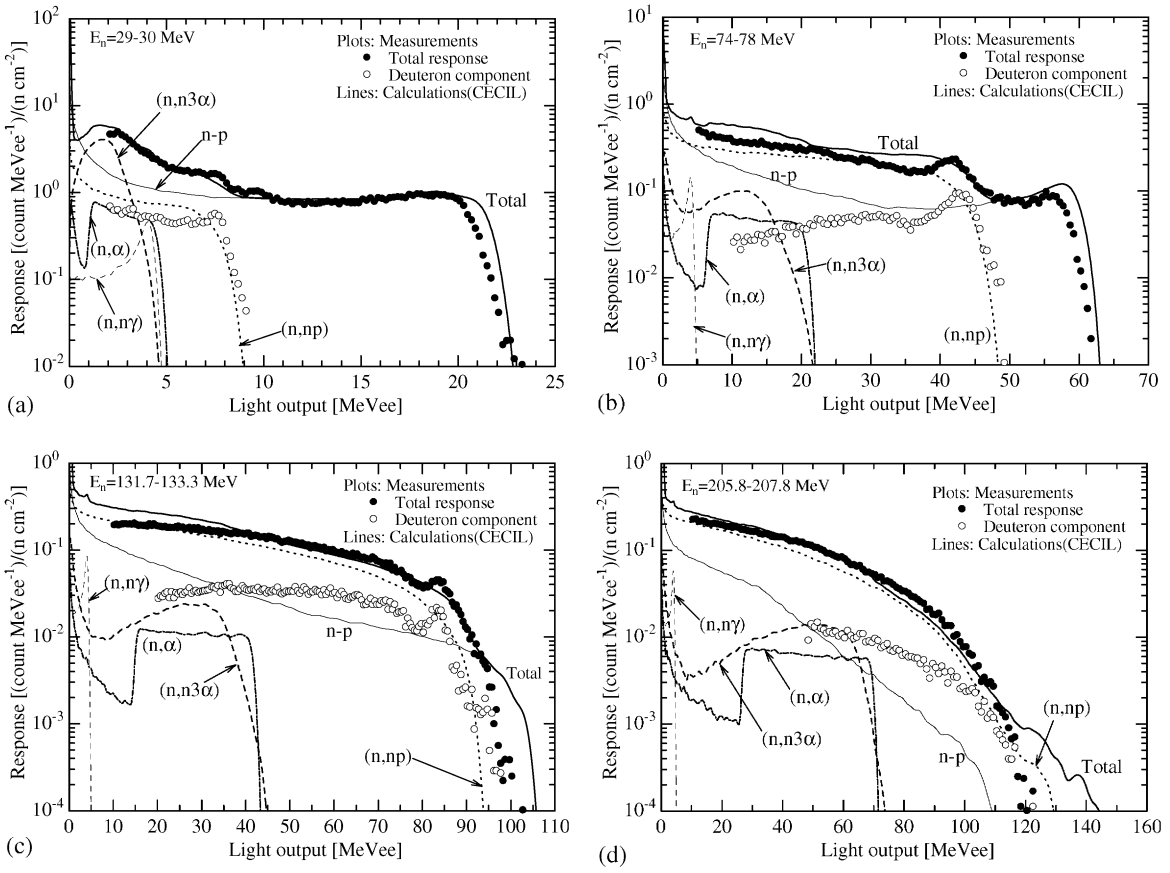

Fig. 7. Summation and components of the light output distributions of particles produced from several neutron reactions in the scintillator for neutron energy ranges of (a) 29–30 MeV, (b) 74–78 MeV, (c) 131.7–133.3 MeV and (d) 205.8–207.8 MeV (Plots: measurement, Lines: calculation). Measured data for (a) and (b) are cited from Ref. [5].

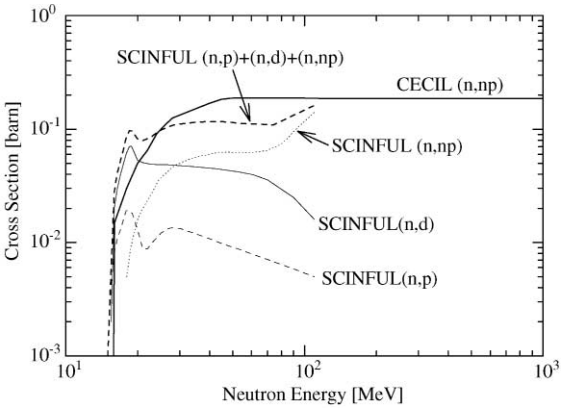

Fig. 8. (n, np) reaction cross-section data compiled in the CECIL code compared with the summation of the (n, d), (n, p) and (n, np) reaction cross-section in the SCINFUL code.

deuterons are similar [5]. Above the neutron energy in which neutron-induced protons and deuterons can escape from the detector wall, however, the difference cannot be neglected because of the range difference between protons and deuterons.

5.2. Wall effect

The measured response functions without escaping protons are also shown in Figs. 6(a) to (i), and are compared with those calculated by the CECIL code modified by excluding the protons escaping from the detector. The minimum light output for the measured total response function

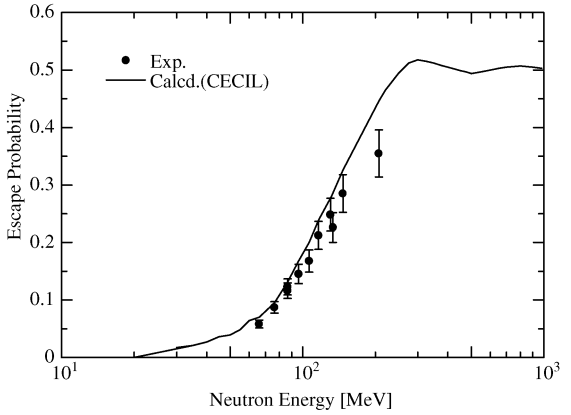

Fig. 9. Ratios of escaping protons to the total efficiencies for a 10 MeVee-threshold compared between measurement and calculations.

including escaping protons is 10 MeVee, because electron events overlap the escaping-proton events below 10 MeVee, as already described above; on the other hand, both electron and escaping-proton events could be discriminated from the other particle events down to the light output of ^{60}Co.

The calculated response functions without escaping protons generally agree well with the measured results, although some difference can be seen in the structure of the response function. Fig. 9 shows the energy dependence of the ratio of escaping-proton event to the total efficiency for 10 MeVee-light-output threshold. This figure indicates good agreement between the experiment and the calculation, it also indicates that the ratio of protons escaping from the detector wall increases with the neutron energy, and that more than 50% of the protons generated in the scintillator of this size cause the wall effect for neutrons above 300 MeV.

5.3. Detection efficiency

Figs. 10(a), (b) and (c) show neutron detection efficiencies which were obtained by integrating the response functions above three thresholds of ^{60}Co (1.15 MeVee), ^{241}Am–Be (4.2 MeVee) and 10 MeVee, respectively. The experimental data by Meigo et al. [14] are also plotted in the figures. Besides, our previous experimental data for 40 and 65 MeV neutrons [15] using 43 and 68 MeV p-^{7}Li quasi-monoenergetic neutron sources at Takasaki Ion Accelerator for Advanced Radiation Application (TIARA), Japan Atomic Energy Research Institute (JAERI) [16] are also shown in the figures. All measured efficiencies in the figures are tabulated in Table 1.

The efficiencies with and without escaping protons calculated by the original and the modified CECIL code, respectively, are shown in the figures for the neutron energy range up to 1 GeV, and the total efficiencies calculated by the SCINFUL code are also shown in the energy range up to 80 MeV, for a comparison with the measured data.

The efficiencies without escaping protons calculated by the modified CECIL code generally agree within a 10–20% difference with those measured in this work at RIKEN. The total efficiencies for 10 MeVee threshold calculated by the original CECIL code also agree within 10% as shown in Fig. 10(c). There seems to be a tendency for a better agreement between the measurement and the calculation by the CECIL code for a higher threshold. On the other hand, the efficiencies calculated by the SCINFUL code generally agree with those measured by Meigo et al. [14] within 10%, but give a big underestimation for a higher threshold.

On the whole, for lower thresholds, such as ^{60}Co and ^{241}Am–Be, the calculated efficiencies by the CECIL code agree comparatively with the measured results for neutron energy higher than 50 MeV, and those by the SCINFUL code do so for that lower than 50 MeV. For the efficiencies of higher thresholds such 10 MeVee, the CECIL code generally agrees with the measurement within 10%.

6. Summary

The response functions of a 12.7 cm diameter by 12.7 cm long NE213 organic liquid scintillator were measured using a quasi-monoenergetic neutron source in the energy range of 66–206 MeV at the RIKEN ring cyclotron facility. The response function without protons escaping from the detector wall induced by high energy neutrons

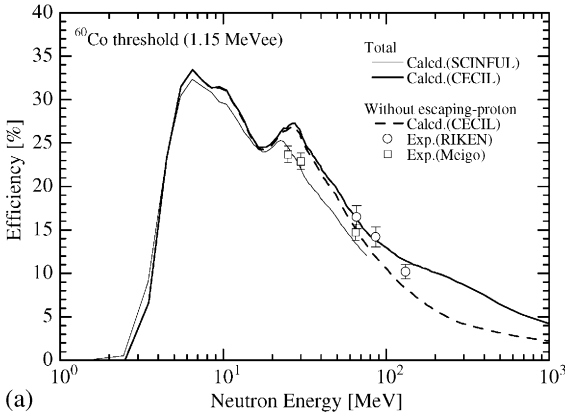

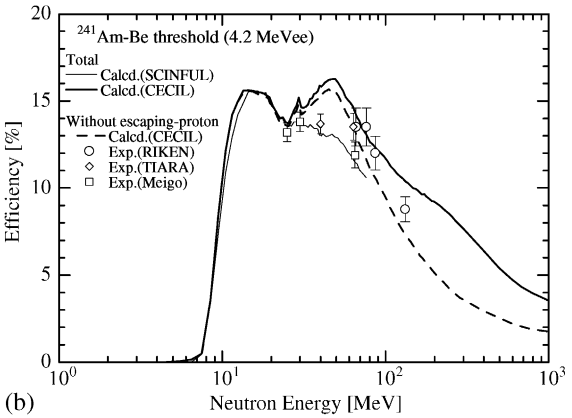

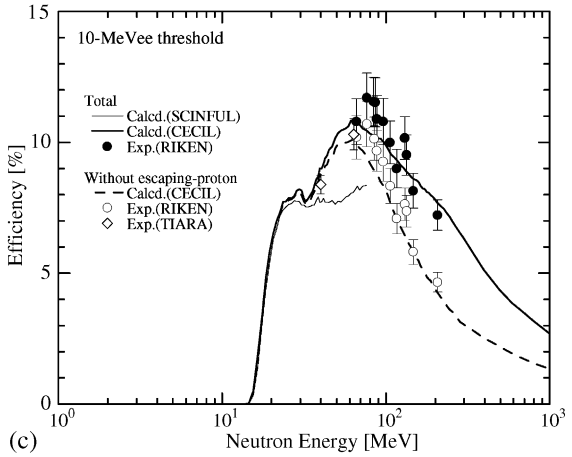

Fig. 10. Neutron detection efficiency of NE213 scintillator for (a) ^{60}Co, (b) ^{241}Am–Be and (c) 10 MeVee threshold. Experimental data are tabulated in Table 1.

Table 1
Measured neutron detection efficiency with and without escaping protons for (a) ^{60}Co, (b) ^{241}Am–Be and (c) (d) 10 MeVee threshold

E_n (MeV)	Efficiency (%)	Relative error	Ref.
(a) *^{60}Co threshold without escaping proton*			
25.0	23.7	0.040	Meigo [14]
65.0	14.7	0.063	Meigo [14]
66.0	16.5	0.081	RIKEN
86.5	14.2	0.081	RIKEN
132.0	10.2	0.081	RIKEN
(b) *^{241}Am–Be threshold without escaping proton*			
25.0	13.2	0.040	Meigo [14]
30.0	13.8	0.041	Meigo [14]
40.0	13.7	0.042	TIARA [15]
65.0	11.9	0.063	Meigo [14]
65.0	13.5	0.058	TIARA [15]
66.0	13.5	0.081	RIKEN
76.3	13.5	0.081	RIKEN
86.5	12.2	0.081	RIKEN
132.0	8.78	0.081	RIKEN
(c) *10 MeVee threshold without escaping proton*			
40.0	8.40	0.042	TIARA [15]
65.0	10.3	0.058	TIARA [15]
66.0	10.2	0.081	RIKEN
76.3	10.7	0.081	RIKEN
86.5	10.1	0.081	RIKEN
86.5	9.68	0.081	RIKEN
96.2	9.27	0.081	RIKEN
106.3	8.34	0.081	RIKEN
116.3	7.09	0.081	RIKEN
132.0	7.64	0.081	RIKEN
132.0	7.37	0.081	RIKEN
146.8	5.82	0.081	RIKEN
206.8	4.66	0.081	RIKEN
(d) *10 MeVee threshold* (*Total*)			
66.0	10.8	0.081	RIKEN
76.3	11.7	0.081	RIKEN
86.5	11.5	0.081	RIKEN
86.5	11.6	0.081	RIKEN
86.5	10.9	0.081	RIKEN
96.2	10.8	0.081	RIKEN
106.0	10.0	0.081	RIKEN
116.3	9.00	0.081	RIKEN
132.0	10.2	0.081	RIKEN
132.0	9.52	0.081	RIKEN
146.8	8.15	0.081	RIKEN
206.8	7.22	0.081	RIKEN

were also estimated, and it was clarified that the ratio of the escaping protons increases from 6% to 35% in neutron energy from 66 to 206 MeV. The response functions with and without escaping proton were calculated using a modified CECIL Monte Carlo code, and the calculated results gave good agreement with the measurements within 10 to 20%.

Acknowledgements

We would like to thank Dr. Takashi Ichihara, Mr. Noriyoshi Nakanishi, Mr. Shin Fujita and Mr. Shunji Nakajima of RIKEN for their help and advise on the experiments. We also thank Dr. Yasushige Yano and other cyclotron staff members for their co-operation in the operation of the pulsed proton beam.

References

[1] V.V. Verbinski, W.R. Burrus, T.A. Love, W. Zobel, N.W. Hill, R. Textor, Calibration of an organic scintillator for neutron spectrometer, Nucl. Instr. and Meth. 65 (1968) 8–25.

[2] J.A. Lockwood, C. Chen, L.A. Friling, D. Swartz, R.N. St. Onge, A. Galonsky, R.R. Doering, Response functions of organic scintillators to high energy neutrons, Nucl. Instr. and Meth. 138 (1976) 353–362.

[3] Y. Uwamino, K. Shin, M. Fujii, T. Nakamura, Light output and response function of an NE-213 scintillator to neutrons up to 100 MeV, Nucl. Instr. and Meth. 204 (1982) 179–189.

[4] K. Shin, Y. Ishii, Y. Uwamino, H. Sakai, S. Numata, Measurements of NE-213 response functions to neutrons of energies up to several tens of MeV, Nucl. Instr. and Meth. A 308 (1991) 609–615.

[5] N. Nakao, T. Nakamura, M. Baba, Y. Uwamino, N. Nakanishi, H. Nakashima, Sh. Tanaka, Measurements of response function of organic liquid scintillator for neutron energy range up to 135 MeV, Nucl. Instr. and Meth. A 362 (1995) 454–465.

[6] J.K. Dickens, SCINFUL: A Monte Carlo based computer program to determine a scintillator full energy response to neutron detecter for E_n between 0.1 and 80 MeV: program development and comparisons of program predictions with experimental data, ORNL-6463, Oak Ridge National Laboratory, 1988.

[7] R.A. Cecil, B.D. Anderson, R. Madey, Improved predictions of neutron detection efficiency for hydrocarbon scintillators from 1 MeV to about 300 MeV, Nucl. Instr. and Meth. 161 (1979) 439–447.

[8] R.C. Byrd, W.C. Sailor, Neutron detection efficiency for NE-213 and BC501 scintillator energies between 25 and 200 MeV, Nucl. Instr. and Meth. A 274 (1989) 494–500.

[9] W.C. Sailor, R.C. Byrd, Y. Yariv, Calculation of the pulse-height response of organic scintillators for neutrons $28 < E_n < 492$ MeV, Nucl. Instr. and Meth. A 277 (1989) 599–607.

[10] N. Nakao, Y. Uwamino, T. Nakamura, T. Shibata, N. Nakanishi, M. Takada, E. Kim, T. Kurosawa, Development of a quasi-monoenergetic neutron field using ^{7}Li(p, n)^{7}Be reaction in the 70–210 MeV energy range at RIKEN, Nucl. Instr. and Meth. A 420 (1999) 218–231.

[11] T. Kurosawa, N. Nakao, T. Nakamura, Y. Uwamino, T. Shibata, N. Nakanishi, A. Fukumura, K. Murakami, Measurements of secondary neutrons produced from thick targets bombarded by high-energy helium and carbon ions, Nucl. Sci. Eng. 132 (1999) 30.

[12] T. Kurosawa, N. Nakao, T. Nakamura, Y. Uwamino, T. Shibata, A. Fukumura, K. Murakami, Measurements of secondary neutrons produced from thick targets bombarded by high-energy neon ions, J. Nucl. Sci. Technol. 36 (1) (1999) 41.

[13] K. Omata, Y. Fujita, N. Yoshikawa, M. Sekiguchi, Y. Shida, A data acquisition system based on a personal computer, INS-Rep.-884, Institute for Nuclear Study, University of Tokyo, 1991.

[14] S. Meigo, Measurements of response function and detection efficiency of an NE213 scintillator for neutrons between 20 and 65 MeV, Nucl. Instr. and Meth. A 401 (1997) 365–378.

[15] N. Nakao, H. Nakashima, T. Nakamura, Sh. Tanaka, Su. Tanaka, K. Shin, M. Baba, Y. Sakamoto, Y. Nakane, Transmission through shields of quasi-monoenergetic neutrons generated by 43 and 68 MeV protons: Part I—concrete shielding experiment and calculation for practical application, Nucl. Sci. Eng. 124 (1996) 228–242.

[16] M. Baba, Y. Nauchi, T. Iwasaki, T. Kiyosumi, M. Yoshioka, S. Matsuyama, N. Hirakawa, T. Nakamura, Su. Tanaka, S. Meigo, H. Nakashima, Sh. Tanaka, N. Nakao, Characterization of a 40–90 MeV ^{7}Li)(p, n) neutron source at TIARA using a proton recoil telescope and a TOF method, Nucl. Instr. and Meth. A 428 (1999) 454.